J Nanopart Res
DOI 10.1007/s11051-010-0011-6

RESEARCH PAPER

Aerosol formation of Sea-Urchin-like nanostructures of carbon nanotubes on bimetallic nanocomposite particles

S. H. Kim · C. Wang · M. R. Zachariah

Received: 21 February 2007 / Accepted: 21 June 2010

Abstract With the advantage of continuous production of pure carbon nanotubes (CNTs), a new simple aerosol process for the formation of CNTs was developed. A combination of conventional spray pyrolysis and thermal chemical vapor deposition enabled the formation unusual sea-urchin-like carbon nanostructures composed of multi-walled CNTs and metal composite nanoparticles. The CNTs formed were relatively untangled and uniform with a diameter of less than ~ 10 nm. The key to the formation of CNTs in this way was to create a substrate particle containing both a catalytic and non-catalytic component, which prevented coking. The density of the CNTs grown on the spherical metal nanoparticles could be controlled by perturbing the density of the metal catalysts (Fe) in the host non-catalytic metal particle matrix (Al). Mobility size measurement was identified as a useful technique to real-time characterization of either the catalytic formation of thin carbon layer or CNTs on the surface of the metal aerosol. These materials have shown unique properties in enhancing the thermal conductivity of fluids. Other potential advantages are that the as-produced material can be manipulated easily without the concern of high mobility of conventional nanowires, and then subsequently released at the desired time in an unagglomerated state.

Keywords Hybrid nanoparticles · Carbon nanotubes · Spray pyrolysis · Thermal CVD

S. H. Kim · M. R. Zachariah (✉)
Nanoparticle-based Manufacturing and Metrology Laboratory, Department of Mechanical Engineering and Chemistry, University of Maryland, College Park, MD 20742, USA
e-mail: mrz@umd.edu

S. H. Kim · M. R. Zachariah
National Institute of Standards and Technology, Gaithersburg, MD 20899, USA

C. Wang
Environmental Molecular Sciences Laboratory, Pacific Northwest National Laboratory, Richland, WA 99352, USA

Present Address:
S. H. Kim
Department of Nanosystem and Nanoprocess Engineering, Pusan National University, 30 Jangjeon-dong, Geumjeong-gu, Pusan 609-735, Korea

Introduction

Carbon nanotubes (CNTs) are generally formed on a supporting transition metal surface (e.g., Fe, Ni, and Co) followed by the diffusion of catalytically formed carbon atoms and subsequent nucleation and growth (Iijima 1991; Andrews et al. 1999; Vander Wal et al. 2000; Cheung et al. 2002). Metal catalysts not only play a major role in supporting the growth of CNTs, but can also be used to control the diameter of

Published online: 27 August 2010

as-grown CNTs (Cheung et al. 2002; Sato et al. 2003). The growth of CNTs can take place either on a substrate (Cheung et al. 2002; Sato et al. 2003) or in the gas phase using free-floating catalysts (Vander Wal et al. 2000; Ci et al. 2000; Ago et al. 2001). For substrate-based growth of CNTs, metal oxide substrates have been used to disperse metal catalysts, and the catalytic properties of metal particles are strongly dependent upon the interactions between substrate and metal particles. In order to minimize the interactions, various oxide materials including silica and alumina were inserted between the substrate and metal particles, resulting in a higher yield of CNTs.

Unlike substrate growth of CNTs, various gas-phase CNT production methods (or floating catalyst method), including laser ablation (Vander Wal et al. 2000; Kim and Zachariah 2005, 2006), wet/dry chemistry (Cheung et al. 2002; Sato et al. 2003), and the HIPCO (Nikolaev et al. 1999) processes were developed with the advantage of the continuous production of high purity CNTs. In those previous aerosol processes, either expensive fabrication approaches (i.e., laser ablation) or complex physical (i.e., high-pressure conditions up to $\sim$10 atm) and chemical processes (i.e., wet/dry chemistry) were needed to produce metal catalysts. One aspect of these processes is that attempting to increase in yields results in soot formation. In particular, hydrocarbons are directly decomposed into amorphous carbon at the CNT growth temperature of $\sim$800 °C, and can coat the nanotubes with amorphous carbon which needs to be removed in a subsequent processing step. Furthermore, the formation of free-floating CNTs has the problem of agglomeration, particularly at high production rates, as well as their possible release into the environment as free highly mobile aerosols with potential human health effects.

In this article, we describe a new, simple, one-step, and inexpensive approach to form pure, highly dense CNTs with a relatively uniform diameter ($<\sim$10 nm) on the surface of large free-flowing metal catalyst particles. This approach has three potential advantages; (1) The use of a large catalyst from which CNT growth should pose less of a hazard because the structure is significantly larger. (2) By anchoring the CNT bundles, aggregation can be minimized by having the option of releasing the CNTs from the large catalyst particle at the desired time and conditions. (3) The CNTs can be released with an acid etch and either directly be suspended in an aqueous solvent, or they can be used in the form of this novel Sea-Urchin (hybrid particle/nanotube structure)-like architecture. In this new approach, a spray pyrolysis method was used to produce aerosol metal catalysts which were decomposed thermally from bimetallic nitrate salts. In this continuous flow process, the aerosol metal catalysts formed were then reacted with acetylene (C_2H_2) in a tube furnace to grow various carbon nanostructures on-the-fly. To our knowledge, this is a new approach in terms of (i) a simple process to produce relatively uniform CNTs on the surface of aerosol metal particles in the gas phase, and (ii) the formation of unusual sea-urchin-like nanostructures composed of CNTs and spherical metal nanoparticles, which can be used as they are, or allow the CNTs to be released, and the catalyst particles removed magnetically or by centrifugation to yield free unagglomerated nanotubes.

Experimental section

Figure 1 shows the schematic of the experimental setup. Two precursor solutions were prepared by (i) dissolving $Fe(NO_3)_3$ non-hydrated in deionized water with a concentration of 3 wt%, and (ii) dissolving $Fe(NO_3)_3$ and $Al(NO_3)_3$ non-hydrated in deionized water with a ratio of 1:1, and a total concentration of 3 wt%.

Iron and composites of iron and aluminum aerosol particles were formed from the thermal decomposition of aqueous solution droplets containing $Al(NO_3)_3$ and $Fe(NO_3)_3$ non-hydrated salt. A Collison nebulizer was employed with a carrier gas flow rate of $\sim$1000 sccm and liquid precursor flow rate of $\sim$0.2 sccm. The carrier gas was nitrogen with the pressure of $\sim$10 psi. The metal nitrates containing aerosol droplets were passed through a silica-gel dryer to remove water so that metal nitrate aerosol particles were formed. Then the dried solid metal nitrate aerosol particles were mixed with a $\sim$75 sccm flow of hydrogen at the entrance of the first tube furnace (50 cm long $\times$ 2.54 cm dia.) heated up to $\sim$1000 °C for the pyrolytic conversion of metal nitrate to the crystalline metal aerosol particles. Both $Al(NO_3)_3$ and $Fe(NO_3)_3$ are known to thermally decompose at $\sim$150 and 125 °C, respectively (Kodas and Hampden-Smith 1999).

Subsequently, the metal aerosol particles formed were introduced into the second tube furnace (60 cm

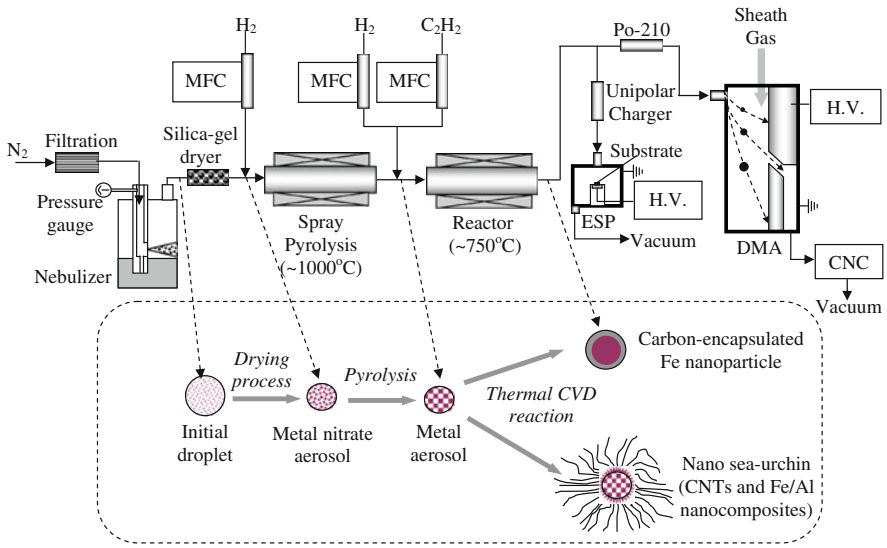

Fig. 1 Schematic of the experimental setup (experimental conditions: (i) $Fe(NO)_3 + H_2O$ [3 wt% solution] for carbon-encapsulated Fe particle, and (ii) $Fe(NO)_3 + Al(NO)_3 + H_2O$ [3 wt% solution, $Fe(NO)_3$:$Al(NO)_3$ = 1:1] for sea-urchin like nanostructured materials (*DMA* differential mobility analyzer; *ESP* electrostatic precipitator; *MFC* mass flow controller; *H.V.* high voltage power supply)

long × 2.54 cm dia.), and reacted with a ~15 sccm flow of acetylene and a ~100 sccm flow of hydrogen at ~750 °C. The gas-phase real-time size distribution measurement of as-grown aerosol materials was done with a differential mobility analyzer (DMA; Model 3081, TSI, Inc.) combined with a condensation nucleus counter (CNC; Model 3025A, TSI, Inc.) (Knutson and Whitby 1975) at the exit of the second tube furnace with the acetylene switched on and off. Before the DMA, the nanostructured aerosol was given a Boltzmann charge distribution by passing them through radioactive ionizing source (Po-210). The charged aerosols were classified by the electrical mobility from a balance of electrostatic and drag forces. The classified aerosol of a given mobility diameter was then subsequently counted with CNC, which grows particles to a size amenable for optical detection particles by the heterogeneous condensation of supersaturated butanol. For TEM analysis, the aerosol grown materials were collected on a TEM grid, by gas-phase electrostatic precipitation to the grid.

Results and discussion

X-ray diffraction (XRD) patterns are shown in Fig. 2 for the metal oxide particles produced by spray pyrolysis at ~1000 °C from a total 3 wt% initial solution composed of iron nitrate and aluminum nitrate with mixing ratios of $Fe(NO_3)_3$:$Al(NO_3)_3$ = 1:0, 1:1, 1:5, and 0:1. The use of a composite particle is essential as will be described later. For the as-produced iron oxide particles in the absence of aluminum oxide (Fig. 2a), the XRD spectrum showed very strong diffraction peaks from iron oxide particles with a crystallite size of ~2 nm estimated using Scherrer's equation (Guinier 1963). However, for the iron and aluminum oxide composite particles (Fig. 2b–d), low-intensity broad XRD peaks were mostly observed, suggesting that (i) the iron oxide (guest) crystallites formed inside aluminum oxide (host) matrix were too small to be detected, or (ii) iron and aluminum oxides were crystallized simultaneously to form a single amorphous phase of $Al_xFe_{(2-x)}O_3$.

The as-produced particles were then mixed with hydrogen to create a reducing environment necessary to remove the oxide layer from the metal oxide particles (i.e., metal core-oxide layer particles), followed by mixing of the hydrocarbon source (C_2H_2) with hydrogen to catalytically grow the carbon nanostructures. In order to verify the gas-phase growth of carbon nanostructures on the metal particles produced by the spray pyrolysis method, a differential mobility analyzer (DMA) combined with a condensation nucleus counter (CNC) was used to obtain a real-time measure of the mobility size distribution of the

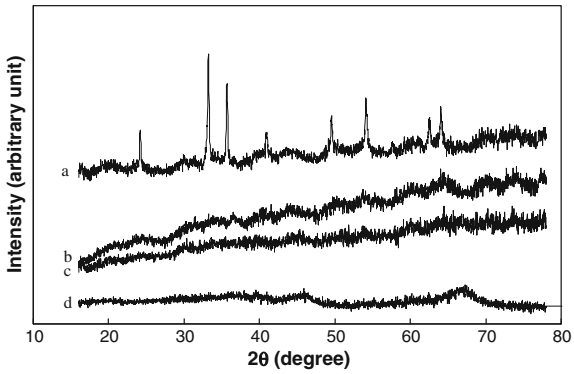

Fig. 2 X-ray diffraction patterns of the metal oxide particles produced by spray pyrolysis (T = 1000 °C) of metal nitrate solution with the mixing ratios of **a** $Fe(NO_3)_3$:$Al(NO_3)_3$ = 1:0, **b** 1:1, **c** 1:5, and **d** 0:1

resulting nanostructured aerosol materials (Kim and Zachariah 2005, 2006; Knutson and Whitby 1975). This enabled real-time monitoring of the size change of the metal composite aerosol particles during nanotube growth. Figure 3 shows the evolution of the size distribution of the metal particles before and after reaction with acetylene. Before acetylene addition, a broad size distribution of either pure Fe particles (Fig. 3a) or composites of Fe and Al particles (Fig. 3b) was observed with a number mean diameter of ~55 nm and geometric standard deviation of ~1.7. After reacting the metal particles with acetylene, the number mean size of the pure Fe aerosol particles increased slightly to ~70 nm. This was attributed to the catalytically induced deposition of amorphous carbon, and the subsequent coking of the iron particle as observed by TEM (see Fig. 4a). On the other hand, growth on the bimetallic Fe and Al nanocomposite aerosols showed a dramatic increase in mobility size of ~200 nm. It should be noted that the DMA measures the mobility size which is related to aerodynamic drag on the particle. Another aspect of the mobility size distributions is that no smaller sized particles (<~20 nm,) were observed as would be expected if the temperatures were high enough to thermally crack the hydrocarbon leading to homogeneous nucleation (Kim and Zachariah 2006). This suggests indirectly that acetylene reacted only heterogeneously with the metal aerosols.

The TEM images presented, Fig. 4a, show reaction with acetylene and hydrogen on the Fe aerosol catalysts, which results in the growth of a thin carbon layer. The mean size of the resulting carbon-

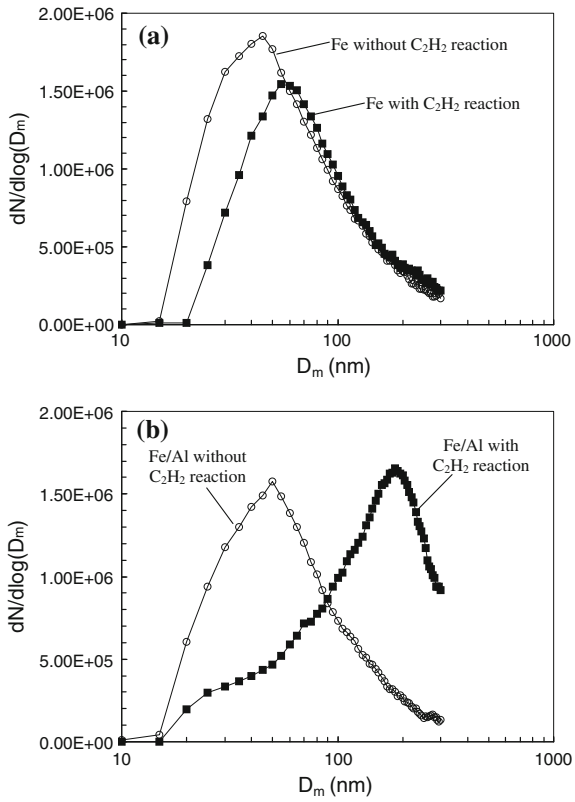

Fig. 3 Evolution of the resulting size distribution of **a** Fe aerosol nanoparticles; and **b** nanocomposite aerosol particles of Fe and Al, before and after the reaction with C_2H_2

encapsulated iron particles was determined using digital image software (Image J, National Institute of Health). The mean core diameter was determined to be ~55 ± 5 nm, which is in agreement with the DMA measurement on the pure unreacted Fe particles (see Fig. 3a). The outer thin carbon layer was determined to be ~10 ± 3 nm, which is consistent with the observed growth (~8 nm) with the DMA upon acetylene addition. Therefore, the catalytic cracking of acetylene leads to catalyst coking. However, as seen in Fig. 4b and c, for the bimetallic Fe and Al aerosol nanocomposites, a dense matting of CNTs with relatively uniform diameter <10 nm was observed over the entire surface of Fe/Al composite particles. While the mechanism is unclear, it is believed that the non-catalytic second phase forces the creation of small iron domains from which the CNTs grow, and more importantly, opens space for the continuous acetylene sequestering of carbon. High resolution TEM (HRTEM) analysis of the CNTs grown on bimetallic aerosol nanoparticles,

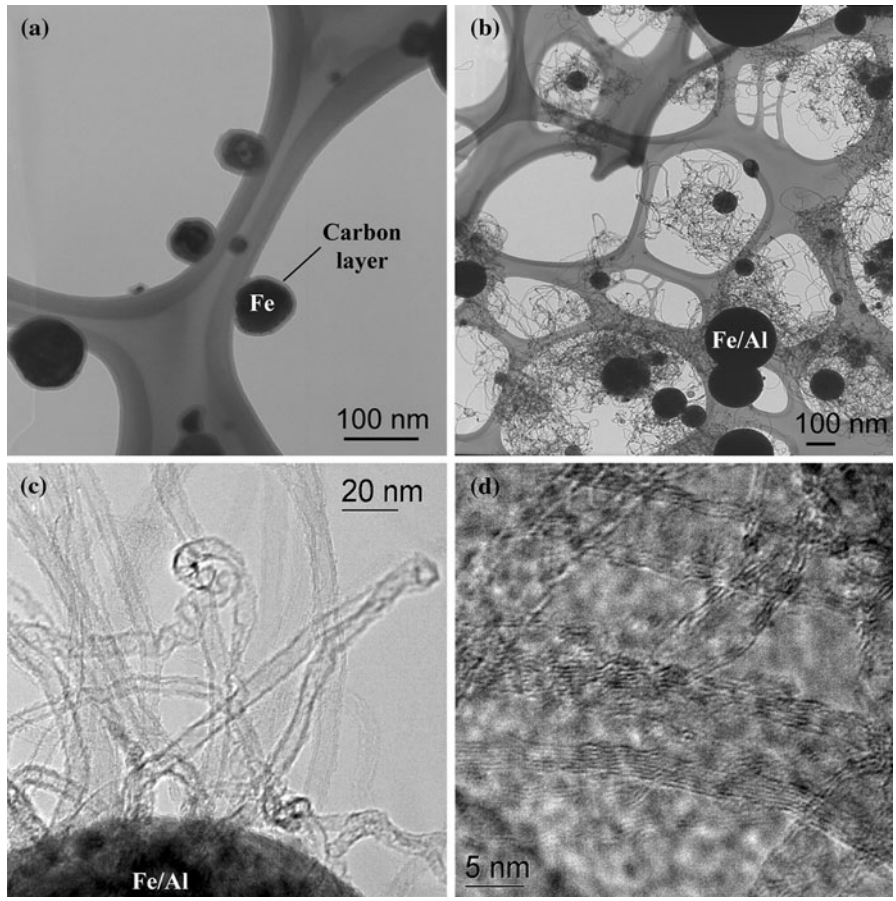

Fig. 4 TEM images of **a** carbon-encapsulated Fe particles, **b**, and **c** carbon nanotubes grown on the surface of the aerosol nanocomposites of Fe and Al, and **d** HRTEM image of carbon nanotubes grown on aerosol nanocomposites of Fe and Al

Fig. 4d, shows multi-wall carbon nanotubes with outer diameter of ~10 nm, and composed of up to ~5 walls and a hollow core.

Of particular interest would be the control of the density of CNTs, which should correlate strongly with the density of the available active Fe sites in the bimetallic Fe/Al nanoparticles. This was tested by creating particles with different Fe/Al ratios by varying the relative metal nitrate precursor concentrations. Figure 5 shows SEM images of the resulting structures, which clearly show the increasing density of CNTs with decreasing Al fraction. Evidently, no CNT growth occurs when the Fe concentration is too low. This condition may result from the nature of the precipitation of the metal nitrate precursors in the droplet, which will also reflect the metal distribution within the final particle (Kodas and Hampden-Smith 1999; Kim et al. 2002). In this case, the solubility of aluminum nitrate is 82 g of $Al(NO_3)_3$/100 g of H_2O is smaller than the solubility of iron nitrate [i.e., 138 g of $Fe(NO_3)_3$/100 g of H_2O], implying that the aluminum nitrate precursor will precipitate out first as water is evaporated from the particle. This precipitation will preferentially occur on the surface of the droplet where the solute concentration is the highest. As such, one should expect Al to be enriched at the surface relative to the Fe, which was found to be necessary for CNT growth and the prevention of coking.

A possible growth mechanism of carbon nanostructures on metal aerosol particles is suggested based on the experimental observations as shown schematically in Fig. 1. During the pyrolysis of the $Fe(NO_3)_3$ aerosol particles, the iron oxide was reduced to pure Fe particles at ~1000 °C in hydrogen, which subsequently reacted with acetylene to create a thin carbon passivation layer (Kim and Zachariah 2006; Massaro and Petersen 1971; Mojica and Levenson 1976). However, for pyrolysis of the $Fe(NO_3)_3$ and $Al(NO_3)_3$ composite, the possible growth pathway is more complicated due to the nature of precipitation. In the early stages of the

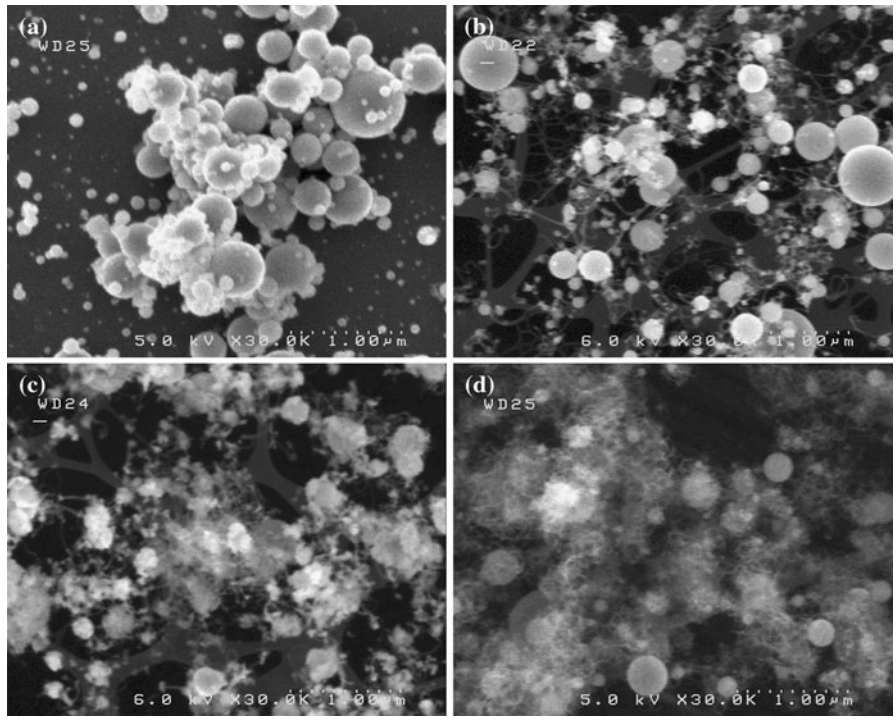

Fig. 5 SEM images of the carbon nanostructures grown on the composite particles with mixing ratios of **a** Fe:Al = 0:1, **b** Fe:Al = 1:5, **c** Fe:Al = 1:2, and **d** Fe:Al = 1:1

drying process (see Fig. 1), the aerosol droplets containing metal nitrate salts lose solvent, and the solute concentration can reach a supersaturated state and begin to nucleate in the droplet. Since solvent evaporation occurs at the droplet surface, the metal nitrate will have the highest concentration. Because $Al(NO_3)_3$ has a lower solubility, an initially 1:1 mixture of the two nitrates will tend to promote more nucleation of Al, resulting in a surface of enriched with Al. Increasing the initial concentration of $Al(NO_3)_3$ relative to $Fe(NO_3)_3$ would further promote surface enrichment of Al and presumably result in a decrease in the size of $Fe(NO_3)_3$ crystals, as well as a corresponding decrease in the Fe catalyst at the particle surface. In this way, one can tune the surface catalyst site through the use of a binary system. After the metal nitrate composite particles were introduced to a hydrogen reducing environment at $\sim$1000 °C, the thermally decomposed metal oxides are reduced to the elemental form of both iron and aluminum. The addition of a hydrocarbon down stream promotes the formation of CNTs with $\sim$10 nm in diameter and a few micrometers in length, at the production rate of $\sim$12 mg/h.

This study also examined the release of CNT from the particle, with the idea that this synthesis pathway might be an effective way of creating relatively untangled CNTs. One of the methods examined was the use of a strong acid (e.g., nitric acid, HNO_3) to etch the metal components. Figure 6a shows a TEM image that the catalyst particles have been removed after the acid treatment. The other advantage of an acid treatment is that it enables us to obtain a homogeneous suspension of CNTs released in a surfactant-free water-based solution, because the nitric acid-assisted chemical oxidation of carbon materials creates a hydrophilic surface structure (Niu et al. 1997; Esumi et al. 1996). This homogeneous CNTs suspension was produced by the guidelines suggested by Choi et al. (2001) and Xie et al. (2003). In brief, 30 mg of urchin-like CNTs was refluxed for 1 h in 40 ml of nitric acid, then filtered, and finally washed to remove any residual acidity. The resulting CNTs collected on the membrane filter were dried at $\sim$100 °C for 4 h and sonicated in DI water for 2 h. These acid-treated CNTs create a stable suspension in water 2–3 months without sedimentation as shown in Fig. 6b.

One application area for the urchin-like structures, which the authors have recently completed is in enhancement of the thermal conductivity of fluids (Han et al. 2006). The nanofluid thermal conductivity

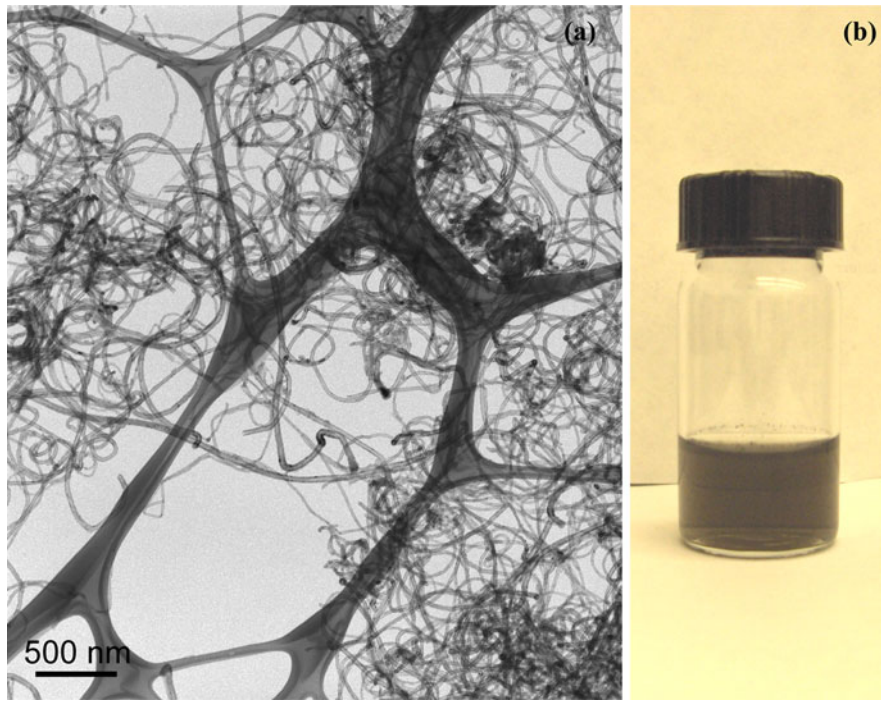

Fig. 6 **a** TEM image of the nitric acid-treated sea-urchin-like CNTs, and **b** nitric acid-treated CNT's suspension after 3 months

in poly-alpha-olefin (PAO) oil measured over a wide temperature ranging from 10 to 90 °C was found to increase the thermal conductivity by 20% at room temperature for volume fractions of the particles <0.2%. This result indicates that these sea-urchin-like particles provide a higher conductivity enhancement when compared to spheres or CNTs at the same loading (e.g., about 13 times higher than spherical alumina nanoparticles for 0.2 vol%). The enhanced thermal conductivity in nanofluids containing sea-urchin-like nanoparticles is attributed to both particle Brownian motion and the high-aspect ratio, and high-thermal conductivity of CNTs.

Conclusions

A new method was used to produce density-controlled and pure CNTs grown on free-flowing metal aerosol nanoparticles. This approach has the combined advantages of an aerosol process, which provides a continuous production method, with those of of a substrate growth approach where the CNTs can be released at the desired time and conditions. By combining conventional spray pyrolysis with thermal CVD processes, relatively uniform multi-walled CNTs with a diameter of less than ~ 10 nm formed on bimetallic aerosol Fe and Al nanocomposites, while only a thin carbon layer was formed on pure Fe aerosol nanoparticles. This new approach has the potential for high-volume production requiring a residence time of <3 s, without soot or amorphous carbon contamination. In addition, the as-produced material can be manipulated easily without concerning the high mobility of conventional nanowires, and then be released at the desired time in a non-agglomerated state. It is also possible that the as-grown sea-urchin-like aerosol nanostructures composed of CNTs and bimetallic nanoparticles can be used directly with potential applications as polymer composites reinforcements, electric conduction, and thermal conduction enhancements.

Acknowledgment This study was supported partially by the NSF-NIRT grant.

References

Ago H, Ohshima S, Uchida K, Yumura M (2001) Gas-phase synthesis of single-wall carbon nanotubes from colloidal

solution of metal nanoparticles. J Phys Chem B 105(43):10453–10456

Andrews R, Jacques D, Rao AM, Rantell T, Derbyshire F, Chen Y, Chen J, Haddon RC (1999) Nanotube composite carbon fibers. Appl Phys Lett 75(9):1329–1331

Cheung CL, Kurtz A, Park H, Lieber CM (2002) Diameter-controlled synthesis of carbon nanotubes. J Phys Chem B 106(10):2429–2433

Choi SUS, Zhang ZG, Yu W, Lockwood FE, Grulke EA (2001) Anomalous thermal conductivity enhancement in nanotube suspensions. Appl Phys Lett 79:2252–2254

Ci L, Li Y, Wei B, Liang J, Xu C, Wu D (2000) Preparation of carbon nanofibers by the floating catalyst method. Carbon 38:1933–1937

Esumi K, Ishigami M, Nakajima A, Sawada K, Honda H (1996) Chemical treatment of carbon nanotubes. Carbon 34:279–281

Guinier A (1963) X-ray diffraction. Freeman, San Francisco, p 124

Han ZH, Yang B, Kim SH, Zachariah MR (2006) Application of hybrid sphere/carbon nanotube particles in nanofluids. Nanotechnology 18:105701–105704

Iijima S (1991) Helical microtubules of graphitic carbon. Nature 354:56–58

Kim SH, Zachariah MR (2005) In-flight size classification of carbon nanotubes by gas phase electrophoresis. Nanotechnology 16:2149–2152

Kim SH, Zachariah MR (2006) In-flight kinetic measurement of the aerosol growth of carbon nanotubes by electrical mobility classification. J Phys Chem B 110:4555–4562

Kim SH, Liu BYH, Zachariah MR (2002) Synthesis of nanoporous metal oxide particles by a new inorganic metrix spray pyrolysis method. Chem Mater 14:2889–2899

Knutson EO, Whitby KT (1975) Aerosol classification by electrical mobility: apparatus, theory, and applications. J Aerosol Sci 6:443–451

Kodas TT, Hampden-Smith MJ (1999) Aerosol processing of materials. Wiley-VCH, New York

Massaro TA, Petersen EE (1971) Bulk diffusion of carbon-14 through polycrystalline nickel foil between 350 and 700 C. J Appl Phys 42(13):5534–5539

Mojica JF, Levenson LL (1976) Bulk-to-surface precipitation and surface diffusion of carbon on polycrystalline nickel. Surf Sci 59(2):447–460

Nikolaev P, Bronikowski MJ, Bradely RK, Rohmund F, Colbert DT, Smith KA, Smalley RE (1999) Gas-phase catalytic growth of single-walled carbon nanotubes from carbon monoxide. Chem Phys Lett 313(1–2):91–97

Niu C, Sichel EK, Hoch R, Moy D, Tennent H (1997) High power electrochemical capacitors based on carbon nanotube electrodes. Appl Phys Lett 70:1480–1482

Sato S, Kawabata A, Nihei M, Awano Y (2003) Growth of diameter-controlled carbon nanotubes using monodisperse nickel nanoparticles obtained with a differential mobility analyzer. Chem Phys Lett 382(3–4):361–366

Vander Wal RL, Ticich TM, Curtis VE (2000) Direct synthesis of metal-catalyzed carbon nanofibers and graphite encapsulated metal nanoparticles. J Phys Chem B 104(49):11606–11611

Xie H, Lee H, Youn W, Choi M (2003) Nanofluids containing multiwalled carbon nanotubes and their enhanced thermal conductivities. J Appl Phys 94(8):4967–4971